

Received: July 17, 1987; accepted: December 7, 1987

Li⁺, F⁻ IONIC MOBILITY IN LITHIUM FLUORIDE GLASSES PREPARED
FROM THORIUM TETRAFLUORIDE (NMR STUDY)

J. SENEGAS

Laboratoire de Chimie du Solide du CNRS, Université de Bordeaux I
351, cours de la Libération, 33405 Talence Cedex (France)

and S.H. PULCINELLI

Instituto de Fisica e Quimica, Universidade de São Paulo,
Campus de São Carlos (U.S.P.), 33560 São Carlos (SP) (Brazil)

SUMMARY

The existence of glasses containing a large amount of LiF (between 25 and 75%) within the ThF₄-LiF binary system has allowed the study of the change in transport properties with LiF content. A ⁷Li and ¹⁹F NMR investigation showed that Li⁺ and F⁻ ions are simultaneously mobile. The temperature dependence of the number of mobile F⁻ ions was determined. In the Li-low concentration domain, transport properties result from contribution of both mobile Li⁺ and F⁻ ions, for high Li concentration they depend only on the Li⁺ ratio. Glasses with high Li content have good electrical performances.

INTRODUCTION

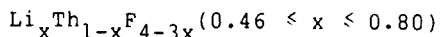
If ZrF₄-based fluoride glasses containing alkali fluorides have been widely studied in the recent past [1,2], research on glasses based on ThF₄ is less developed [3,4,5]. The difficulty

to vitrify these materials is now overcome by using the hyper-quenching technique which allows synthesise them in a large range of composition. There is an increasing interest in new fluoride glasses because of their potential use for infrared optical components and ultra-low optical fibers. On the other hand they are cationic (Li^+) and anionic (F^-) conductors. The possibility of incorporating large amount of lithium fluoride allows an NMR study of the influence of the LiF ratio on the electrical properties of glasses belonging to the binary LiF-ThF₄ system : this technique leads to the determination of the nature and the number of carriers for each composition. An I-R study, pursued simultaneously, allows us to relate the conduction properties to the coordination of the thorium in the network.

GLASS PREPARATION

The starting materials are LiF (commercial product) and ThF₄. ThF₄ is obtained from ThO₂ using a 40% HF solution at 100°C and followed by gas anhydrous HF for 4 hours at 500°C. The mixed fluoride components are pressed into pellets and heated to melting in a nickel crucible under an argon atmosphere. The glass preparation has been carried out in open crucible using the 'splat roller' quenching procedure which has been described elsewhere [6]. The quenching speed attains 10^6Ks^{-1} and the quenching temperature, depending on the compositions of samples varies between 800 and 1100°C.

The compositions of glasses obtained in the binary LiF-ThF₄ system are, in accordance with the eutectic region observed in the phase diagram [7], the following :



Hydrolysis and thermal properties studied elsewhere [5] show that these samples are stable at room atmosphere and also in aqueous solutions at 20°C. The transition (T_G) and crystallisation (T_C) temperature of some studied glasses are collected in Table I.

Table I

Number of sample, x value, composition (mole % and global), glass transition temperature T_G (K) and crystallization temperature T_C (K)

Sample	x	Composition	Global composition	T_G (K)	T_C (K)
1	0.80	$\text{Li}_{0.80}\text{Th}_{0.20}\text{F}_{1.60}$	$\text{MF}_{1.60}$	485	496
2	0.75	$\text{Li}_{0.75}\text{Th}_{0.25}\text{F}_{1.75}$	$\text{MF}_{1.75}$	496	500
3	0.70	$\text{Li}_{0.70}\text{Th}_{0.30}\text{F}_{1.90}$	$\text{MF}_{1.90}$	514	529
4	0.65	$\text{Li}_{0.65}\text{Th}_{0.35}\text{F}_{2.05}$	$\text{MF}_{2.20}$	504	518
5	0.60	$\text{Li}_{0.60}\text{Th}_{0.40}\text{F}_{2.20}$	$\text{MF}_{2.20}$	504	518
6	0.54	$\text{Li}_{0.54}\text{Th}_{0.46}\text{F}_{2.98}$	$\text{MF}_{2.38}$	*	*

* not available

The samples were monitored by EPR: the presence of small amounts (about 10 ppm) of paramagnetic impurities (Mn^{2+} , Cu^{2+}) were revealed in some compositions. Susceptibility determination at 21°C with a Faraday balance shows that these samples exhibit a weak paramagnetism. All the other compositions are diamagnetic.

NMR INVESTIGATIONS

Experimental methods

C.W. NMR measurements have been performed on ^{19}F and ^7Li nuclei over the temperature range 170-450K (i.e. between -100°C and 180°C) on the various samples of Table I.

The 30 Mhz frequency used allowed us to record under the same conditions the absorption signals of fluorine (at 7500G) and of lithium (at 18130G). The very good signal/noise ratio obtained leads to weak modulation fields and avoids data corrections.

From the resonance spectra three types of informations have been collected and analyzed:

1) the surface of the integrated line shape which is proportional to the number of resonance nuclei. When there is a partial overlapping of the two curves corresponding to mobile and non mobile nuclei, deconvolution allows an evaluation of each contribution.

2) the temperature dependence of the fluorine and lithium line-width (the measured peak to peak linewidth is called ΔH_{pp})

3) the experimental second moment (M_{2exp}), corrected eventually by the modulation factor. A computer treatment of the data collected gives a value of M_{2exp} from the expression:

$$M_{exp} = \frac{\int_{-\infty}^{+\infty} h^3 g'(h) dh}{\int_{-\infty}^{+\infty} h g'(h) dh}$$

where h is the algebraic deviation (in Gauss) from the resonance field and $g'(h)$ the derivated signal recorded.

Results

a) Lithium resonance

The thermal evolution of the resonance line shape of ${}^7\text{Li}$ exhibit for all the compositions the behavior illustrated in Fig.1, for the sample 1. No quadrupolar effect can be detected but there is a continuous line narrowing up to the highest experimental temperature. The linewidth evolution of all the samples are given in Fig.2 : the linewidth, constant at low temperature in the rigid lattice range, decrease above a temperature $T_{A_{Li}}$ (K). The $T_{A_{Li}}$ temperature of the samples and the rigid lattice linewidth value denoted $(\Delta H_{pp}^R)_{Li}$ are given in Table II . The line narrowing occurs when the lithium jump frequency ν_{Li} is of the order of $(\Delta \nu_{pp}^R)_{Li}$. $(\Delta \nu_{pp}^R)_{Li}$ is the value of corresponding $(\Delta H_{pp})_{Li}$ expressed in Hz.

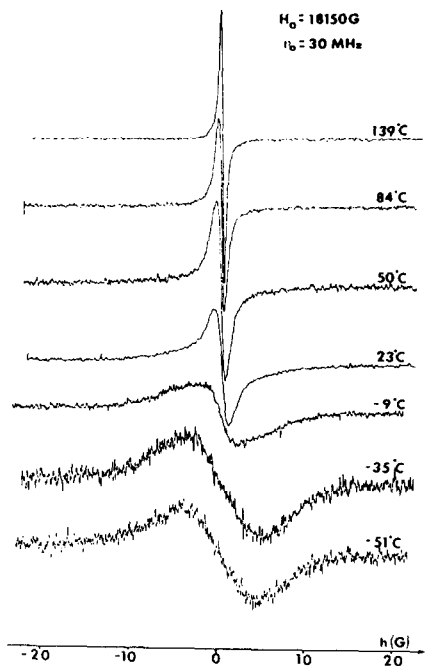


Fig. 1. Thermal evolution of ${}^7\text{Li}$ NMR line shape for the sample 1 ($\text{Li}_{0,80}\text{Th}_{0,20}\text{F}_{1,60}$).

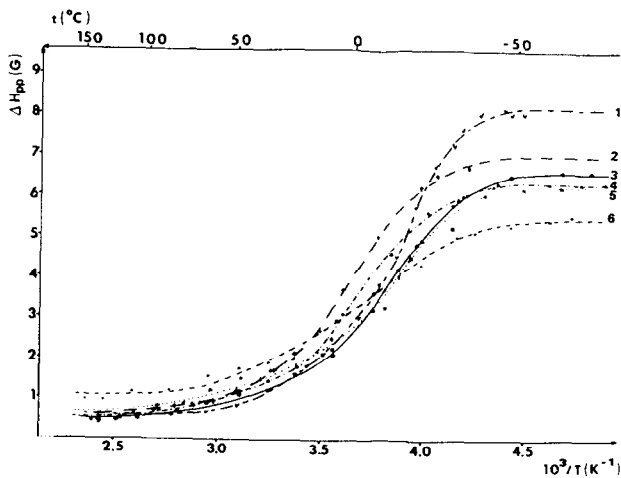


Fig. 2. Thermal evolution of ${}^7\text{Li}$ linewidth ΔH_{PP} (G) for all the glasses.

Table II

Temperature of the ${}^7\text{Li}$ motional narrowing beginning $T_{A, \text{Li}}$ (K), transition temperature T_R (K) (see text), ${}^7\text{Li}$ rigid lattice linewidth ΔH_{pp} (G), activation energy upon $T_R : \Delta E_{\text{Li}}^1$ (eV) and under $T_R : \Delta E_{\text{Li}}^2$ (eV)

sample	composition	$T_{A, \text{Li}}^1$ (K)	T_R (K)	$(\Delta H_{pp}^R)_{\text{Li}}$ (G)	ΔE_{Li}^1 (eV)	ΔE_{Li}^2 (eV)
1	Li _{0.80} Th _{0.20} F _{1.60}	231	256	8.2	0.19	0.37
2	Li _{0.75} Th _{0.25} F _{1.75}	239	276	7.0	0.18	0.32
3	Li _{0.70} Th _{0.30} F _{1.90}	231	280	6.6	0.13	0.23
4	Li _{0.65} Th _{0.35} F _{2.05}	231	290	6.3	0.12	0.21
5	Li _{0.60} Th _{0.40} F _{2.20}	225	261	6.2	0.11	0.33
6	Li _{0.54} Th _{0.46} F _{2.38}	223	263	5.5	0.11	0.26

The thermal variation ν_s can be deduced from that of $(\Delta\nu_{pp})_{Li}$ from the expression [8].

$$\nu_s = \frac{\alpha \Delta\nu_{pp}}{\text{tg} \left[\pi/2 \left(\frac{\Delta\nu_{pp}}{\Delta\nu_R} \right)^2 \right]}$$

The α constant, characterizing the line shape, is chosen as 1 according to the nearly gaussian shape of the line at low temperatures. ν_s presents a temperature activated behavior as follows:

$$\nu_s = \nu_0 \exp(-\Delta E/kT)$$

In the temperature range of the lithium motional narrowing the fluorine motions do not affect the lithium line shape. Therefore the activation energies ΔE_{Li} relative to the lithium mobility can be deduced from $\ln \nu_s$ v.s. T^{-1} plots presented in Fig. 3. The two linear parts of each evolution are separated by a break at temperature T_R . Two activation energies can be deduced from the two slopes: ΔE_{Li}^1 above T_R and ΔE_{Li}^2 under T_R . These values are collected in Table II.

b) Fluorine resonance

The thermal evolution of the fluorine line shape is given for sample 1 on Fig. 4. All the other samples studied show similar behavior. At low temperature only a broad line can be observed. At increasing temperature, above T_{AF} , a narrow line characterizing mobile fluorines, appears and grows at the expense of the broad one. Extreme narrowing cannot be reached at the highest temperature T_{BF} explored (limited to about 420 K because of the proximity of T_G). The temperatures T_{AF} and T_{BF} are listed in Table III.

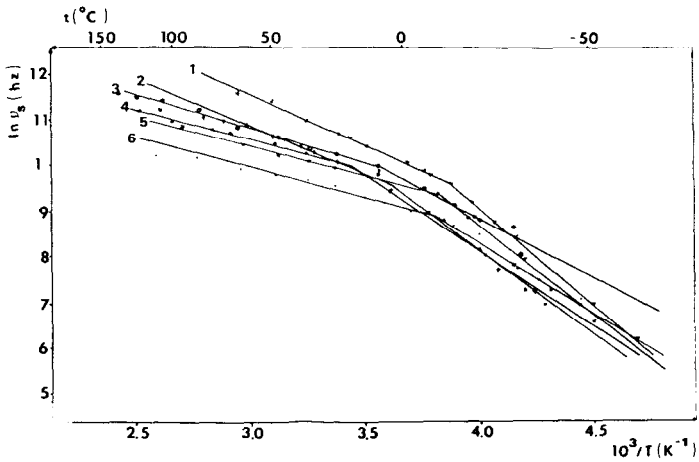


Fig. 3. Thermal evolution of ${}^7\text{Li}$ jump frequency ν_s (semilogarithmic scale).

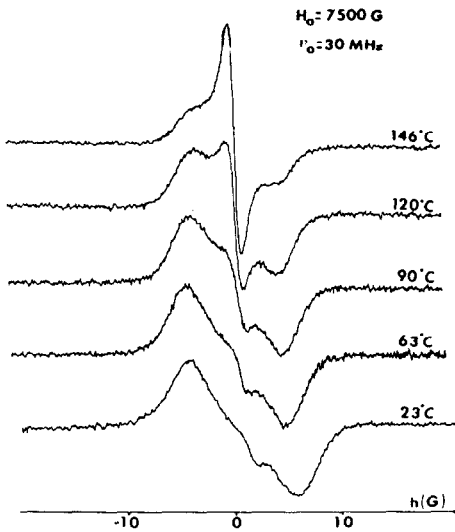


Fig. 4. Thermal evolution of ${}^{19}\text{F}$ NMR line shape for the sample 1 ($\text{Li}_{0.80}\text{Th}_{0.20}\text{F}_{1.60}$).

Table III

Temperature of ^{19}F motional narrowing beginning T_{AF} (K), highest temperature for the determination of mobile fluoride T_B (K), proportion of mobile fluoride f (%), number of mobile fluoride (per total cation number equal 1) N_{mf} , limits ΔE_A and ΔE_B (eV) of the distribution domain of activation energy of fluoride mobility, width $\Delta E_B - \Delta E_A$ (eV) and center $(\Delta E_A + \Delta E_B)/2$ (eV) of the distribution domain

SAMPLE	COMPOSITION	T_{AF} (K)	T_B (K)	f (%)	N_{mf}	ΔE_A (eV)	ΔE_B (eV)	$\Delta E_B - \Delta E_A$ (eV)	$(\Delta E_A + \Delta E_B)/2$ (eV)
1	$\text{Li}_{0.80}\text{Th}_{0.20}\text{F}_{1.60}$	289	420	25.5	0.38	0.19	0.34	0.15	0.265
2	$\text{Li}_{0.75}\text{Th}_{0.25}\text{F}_{1.75}$	287	414	12.0	0.27	0.12	0.25	0.13	0.185
3	$\text{Li}_{0.70}\text{Th}_{0.30}\text{F}_{1.90}$	293	417	13.5	0.26	0.10	0.21	0.11	0.155
4	$\text{Li}_{0.65}\text{Th}_{0.35}\text{F}_{2.05}$	278	415	12.0	0.25	0.12	0.22	0.10	0.170
5	$\text{Li}_{0.60}\text{Th}_{0.40}\text{F}_{2.20}$	279	420	12.5	0.21	0.10	0.21	0.11	0.155
6	$\text{Li}_{0.54}\text{Th}_{0.46}\text{F}_{2.38}$	281	435	11.0	0.25	0.09	0.20	0.11	0.145

DISCUSSION

Lithium mobility

The continuous narrowing of the lithium line shape indicates that all the Li^+ ions are mobile above T_{ALi} (230 K). Activation energies ΔE_{Li}^2 ($T < T_{\text{R}}$) are two or three times higher than ΔE_{Li}^1 ($T > T_{\text{R}}$) (Table II). This surprising result, may be explained if ΔE_{Li}^2 values are supposed to take into account the dissociation energy of LiF into separate ions Li^+ and F^- . This separation requires a lower energy in a glass than in an ionic crystal. Transition temperature T_{R} may be connected to a change in the conduction process from short to a long range transport. A certain degree of crystallisation is observed in samples 1 and 5. This can explain the dispersion in the high values of ΔE_{Li}^2 found for these two compositions.

ΔE_{Li}^1 decreases with the lithium concentration (Table II). Diffusion coefficients D_2 may be calculated according to the relation: $D = \frac{\langle \lambda \rangle^2}{6} \nu$ [9] valid for an isotropic lithium diffusion. ν corresponds to the Li^+ jump frequency $\nu_{\text{S}, \langle \lambda \rangle}^2$ is the mean square distance between two jumps of Li^+ . A value of $\lambda = 3 \text{ \AA}$ is deduced from the Li-Li distance in the crystallized compound Li_3ThF_7 [10]. A significant value of D is calculated as 400 K and denoted D_{400} . Its variation with lithium concentration, given on Fig. 5, exhibits a constant increase with the lithium ratio becoming drastic for the composition 1.

Fluoride mobility

As is illustrated in Fig. 6, only a fraction f of the fluorine is mobile. f increases with temperature and can be determined, at a given temperature, from the ratio of the integrated surfaces of the narrow and the broad fluorine resonance lines. Fig. 6 reports the thermal variation of $f = m/m+s$ (where m and s refer respectively to the number of mobile (m) and static (s) fluorine nuclei) for all investigated glasses. The values of f

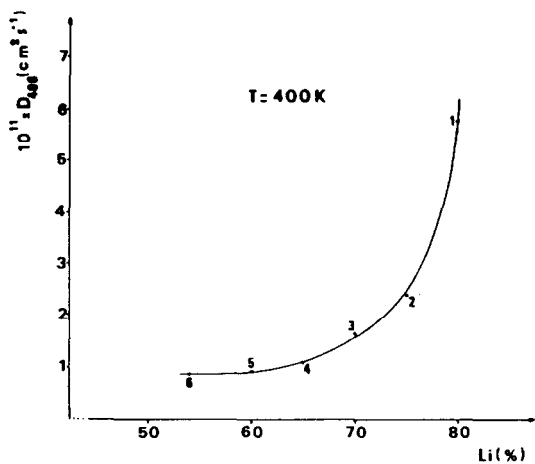


Fig. 5. Variation of the lithium diffusion coefficient D ($\text{cm}^2 \text{s}^{-1}$) with lithium concentration.

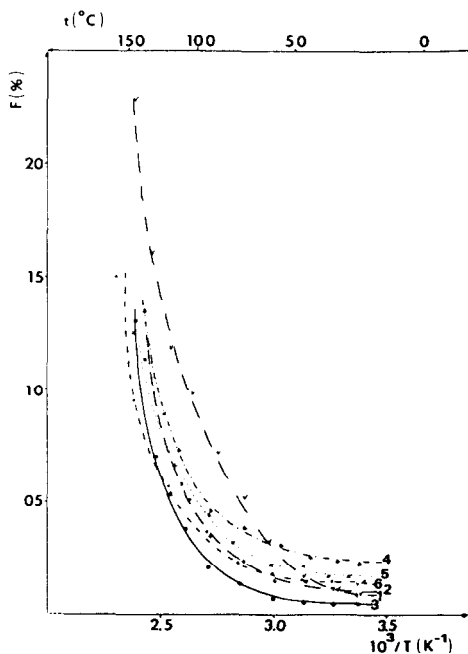


Fig. 6. Variation of the fraction f (%) of mobile fluoride with temperature.

at T_{BF} and N_{mF} (N_{mF} is the number of mobile fluoride ions per total F cation number equal to 1) are given in Table III. Only a small part of the fluoride ions are mobile, even at high temperature. Varying between 12% and 13% for samples, 2 to 6, this proportion reaches 25% for the sample 1.

$Li_{0.75}Th_{0.25}F_{1.85}$ appears as a boundary composition in the glass domain (this vitreous composition exists also as a crystallized phase Li_3ThF_7): about 1/7 of fluorine anions are mobile in this phase. For the lower Li-concentration compositions the number of mobile fluorides is quasi constant and less than 1/7 of fluorine by formula is mobile.

On the contrary for the richest Li-concentration 1 ($Li_{0.80}Th_{0.20}F_{1.60}$) the number of mobile fluoride drastically increases and reaches about double the preceding quantity. This result seems to be connected to the change in the thorium coordination numbers which increases when the lithium ratio increases (confirmed by the IR measurements). It implies that the strength of the Th-F bond decreases and consequently that the number of mobile fluorides increases with lithium concentration.

Another interesting result is the increasing ratio of mobile fluoride with temperature (Fig. 6). It involves several energy levels in the glasses. Several distributions of activation energies have been investigated using the same model as in a previous work [11] on such glasses. A broad and flat distribution leads to the best fit of the points of Fig. 6. The values of the activation energy limits of this distribution ΔE_A and ΔE_B , of the distribution widths ($\Delta E_A - \Delta E_B$) and of the mean values of these energies ($\frac{\Delta E_A + \Delta E_B}{2}$) are gathered in Table III.

INFRARED MEASUREMENTS

Infrared transmission spectra were recorded for all the samples, in polyethylene pressed-discs (30 mg $(C_2H_4)_n$ / 3mg glass), in a Perkin-Elmer 983 double beam spectrometer above 180 cm^{-1} , 3 cm^{-1} resolution at room temperature.

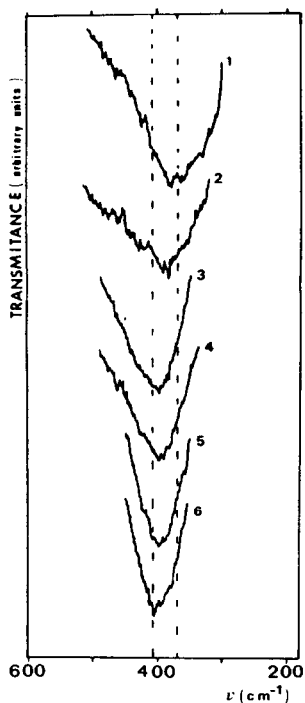


Fig. 7. Variation of the Th-F frequency $\nu_{\text{Th-F}}$ (cm^{-1}) with composition (transmission I.R. spectra).

Figure 7 reports I.R. spectra of all the glasses, showing main peak which is structure sensitive, as its frequency varies with glass composition between 380 and 410 cm^{-1} . According to previous work [12], there is a strong correlation between an increase in coordination number and a decrease in the frequency of the dominant IR band, due to a decrease in bond strength which lowers the value of the force constants. In the case of crystalline Li_3ThF_7 , the Th atoms are in 9-fold coordination [10] and the vibration frequency is displaced to 390 cm^{-1} .

The structural interpretation proposed for the glass samples is the following : the thorium environment is roughly maintained, the coordination number of Th increases from a value lower than 9 for the sample 1 to values greater than 9 for the samples 3, 4, 5, 6 .

CONCLUSION

In the glass domain $\text{Li}_x\text{Th}_{1-x}\text{F}_{4-3x}$ ($0.46 \leq x \leq 0.80$), conduction properties are supported by both lithium and fluoride ions. All the lithium cations are mobile and mainly responsible for the conductivity. On the contrary, only a small part of fluoride anions, increasing with temperature, participates to the conduction. For samples 2 to 6 (low Li-concentration) the quantity of mobile fluoride is quasi-constant but an important increase is observed in the case of sample 1 (highest Li-concentration): a phenomenon connected with a correlative increase of thorium coordinance.

ACKNOWLEDGEMENTS

One of us (S.H.P.) thanks the CNPq (Conselho Nacional de Desenvolvimento Científico e Tecnológico - Brasil) for the support provided by a grant n° 200.301/84-QU.

REFERENCES

- 1 M. POULAIN, M. POULAIN and C. LUCAS, *J. Rev. Chem. Miner.* 16, 267 (1979).
- 2 A. LECOQ, M. POULAIN, *J. Non-Cryst. Solids*, 34, 101 (1979).
- 3 M. POULAIN and M. POULAIN, *J. Non-Cryst. Solids*, 56, 57 (1983).
- 4 J.M. REAU, J. SENEGAS, H. AOMI, P. HAGENMULLER and M. POULAIN, *J. Solid State Chem.*, 60, 159 (1985).
- 5 H.W. SUN, B. TANGUY, J.M. REAU and J. PORTIER, *J. Solid State Chem.*, 63, 191 (1986).
- 6 M. POULAIN, M. POULAIN, J. LUCAS, Brevet ANVAR n°770 618, US Pat. n° 4 141 741.

- 7 R.E. THOMA, M. INSLUY, B.S. LANDAU, M.A. FRIEDMAN and W.R. GRIMES, J. Phys. Chem., 63, 1267 (1959).
- 8 F.A. RUSHWORTH and D.P. TUNSTALL, 'Nuclear Magnetic Resonance', Gordon and Breach, New York (1961).
- 9 Jr. R.C BOWMAN, R.C. ATTALA and W.E. TADLOCK, Int. Hydrogen Egy, 1, 421 (1977).
- 10 S.H. PULCINELLI (to be published).
- 11 J. SENEGAS, J.M. REAU, H. AOMI, P. HAGENMULLER and M. POULAIN, J. Non-Cryst. Solids, 85, 3, 315 (1986).
- 12 R.M. ALMEIDA, J.D. MACKENZIE, J. Chem. Phys., 78 (11) 6502 (1983).